Astronomical and Astrophysical Transactions (*AApTr*), 2025, Vol. 35, Issue 3, pp. 325–332,
ISSN 1055-6796, Photocopying permitted by license only, ©Cambridge Scientific Publishers

Solar flare classes and interplanetary type II bursts dependence of solar cycles 23–25

Diyorbek Pulatov*, Zavkiddin Mirtoshev

Department of Nuclear Physics and Astronomy, Samarkand State University, 140104 Samarkand, Uzbekistan

Received 27 April, 2025; accepted 30 May, 2025

This study shows the correlation of 705 interplanetary (IP) type II radio bursts detected during the solar cycle (SC) 23, 24, and ascending phase of SC 25 with sunspot number (SSN) and number of flares by class. The results show that 675 (96%) of these bursts were associated with coronal mass ejections (CMEs), while the remaining 30 (4%) were not associated with CMEs. The total number of IP type II bursts was caused by B-class (5), C-class (138), M-class (275), and X-class (124) solar flares, and among them, M-class (51%) flares dominated. We examined the relationship between IP type II bursts and SSN during the ascending phase of all three SCs and found a high correlation between them (correlation coefficients 0.91, 0.98, 0.99, respectively). We found the correlation of the number of IP type II bursts with the number of C, M, and X solar flares, and found that M-class flares showed a strong correlation with IP type II bursts (correlation coefficients 0.76, 0.93, and 0.72, respectively)

.

Keywords: Interplanetary radio burst, CME, solar cycle, solar flare, space weather

1 Introduction

CMEs are giant clouds of magnetized plasma that are ejected from regions of the Sun's magnetic field into IP space. CMEs can be powerful drivers of plasma ejections that can accelerate electrons to high energies (Webb & Howard 2012). Three types of low-frequency solar radio bursts (SRBs) are caused by the acceleration of non-thermal electrons. Radio bursts propagate into the IP environment with energetic CMEs and affect the Earth if they are directed towards the Earth. SRBs are divided into five different types based on their origin and frequency range (Gopalswamy 2016). Type I radio bursts are noise storms observed in the high-frequency range. Slow drift type II bursts are remarkable phenomena associated with high-energy flares. They are thought to be plasma emissions produced by a shock wave propagating in the solar

*Email: diyorbekpolatov2002@gmail.com

corona. Type III bursts are primarily produced by electrons accelerated along open magnetic field lines in the lower solar corona. They are characterized by a rapid drift from high to low frequencies in the short-term dynamic spectrum. Type IV bursts are the continuous radiation that follows a type II burst. Type V bursts are a diffuse extension (typically below 150 MHz) of the broadband continuum following a type III burst. It is thought to be the emission of electrons that caused the type III burst to be trapped in a magnetic loop (Pick & Vilmer 2008). Typically, the diffuse structure surrounding the CME flux rope is considered to be the shock that produces a type II burst. Therefore, it is important to study the relationship of type II bursts to CMEs and the SC. Several scientists have studied the relationship between type II bursts, the SC and flare class. Patel et al. (2021) divided decametric–hectometric (DH) type II bursts into three groups based on frequency rate and studied their dependence on the SC and CMEs occurrence rate. The majority of DH type II bursts occurrence in SC 23 correspond to the high frequency group 158 (47%). Kumari et al. (2023) also studied the relationship between the type II bursts and the CME types (Halo and Partial Halo) observed in SC 23 and 24. Total type II bursts observed in SC 23 and 24, 144 (23.6%) and 108 (26%) were produced by Halo CMEs respectively. Studying the formation of solar radio bursts is of great importance for coronal plasma diagnostics.

In this paper, we investigated the SC dependence of IP type II bursts caused by three types of flares. We calculated the correlation coefficient between each type of flare number and SSN during SC 23, 24 and the ascending phase of SC 25.

2 Observational data

In this study, we used the IP type II burst catalog[1] observed using the WIND/WAVES and STEREO/WAVES spacecraft. This catalog includes CMEs associated with IP type II events, along with additional information about source region parameters such as heliographic coordinates, active region number, and flare class. WAVES has been continuously monitoring low-frequency radio emissions from the Sun since its launch in the 20 kHz – 14 MHz frequency range. We identified 705 IP type II bursts on the Wind catalog from 1996 to 22 September 2024 and checked their association with flares and used the SSNs provided by the SILSO World Data Center[2] (1996–2024). In these studies, we investigated the dependence of IP type II bursts on the solar cycle and found that the number of flares by class that produced IP type II bursts were linear correlated to the SSN.

3 Results and discussion

Type II radio bursts are produced by non-thermal electrons and occur at radial distances of 1–2 $R_{\odot}$. They usually represent a decrease in electron density in the fundamental and harmonic structure as it slowly shifts from high frequency to low frequency.

[1] https://cdaw.gsfc.nasa.gov/CME_list/radio/waves_type2.html
[2] https://www.sidc.be/SILSO/datafiles

Table 1 The number of IP type II radio bursts and the number of flare classes with different characteristics.

Year	SSN	Halo CME numbers	IP type II burst number	Flare classes			
				B	C	M	X
1996	11.6	–	1	–	–	–	–
1997	28.9	4	12	1	4	3	3
1998	88.3	9	31	2	6	10	6
1999	136.3	8	21	–	5	8	2
2000	173.9	30	53	–	11	25	9
2001	170.4	29	55	–	7	24	15
2002	163.6	28	53	–	9	27	6
2003	99.3	17	33	–	3	9	13
2004	65.3	14	33	–	10	16	2
2005	45.8	32	40	–	5	11	12
2006	24.7	6	13	–	4	3	4
2007	12.6	1	3	1	2	–	–
2008	4.2	–	2	1	–	1	–
2009	4.8	–	–	–	–	–	–
2010	24.9	1	3	–	2	1	–
2011	80.8	17	29	–	6	14	4
2012	84.5	22	28	–	5	11	5
2013	94	21	39	1	11	10	6
2014	113.3	28	45	–	7	15	4
2015	69.8	14	23	–	5	14	1
2016	39.8	1	4	–	1	1	–
2017	21.7	6	9	–	1	2	2
2018	7	–	1	–	–	–	–
2019	3.6	–	1	–	1	–	–
2020	8.8	2	2	–	1	1	–
2021	29.6	6	15	–	5	6	1
2022	83.2	14	34	–	8	19	2
2023	125.5	31	55	–	14	17	7
2024	154.7	41	68	–	5	28	20

Table 1 presents the annual distribution of SSN and IP type II radio bursts and the number of flares by class and Halo CMEs that caused the radio bursts. During the SC 23, 24 and ascending phase of SC 25, 705 IP type II bursts were reported. The annual number of IP type II bursts has shown a strong correlation with the SC. Also Kumari et al. (2023) divided type II bursts into associated and not associated by CMEs during SC 23, 24. Type II bursts accompanied by CMEs showed a strong correlation with SC 23 and 24, correlation coefficients are $cc = 0.94$ and $cc = 0.98$, respectively. Type II bursts associated with CMEs showed 79% and 95% correlation in SC 23 and SC 24 respectively.

Studies by Patel et al. (2021) also divided DH type II bursts in SC 23 and 24 into three groups: low frequency (20 kHz – 200 kHz), medium frequency (200 kHz – 1 MHz) and high frequency (1 MHz – 16 MHz). They studied the importance of frequencies in generating the burst and found that 49% of DH type II bursts in SC 23 and 24 occurred at frequencies below 1 MHz. It is noteworthy that the events occurring at

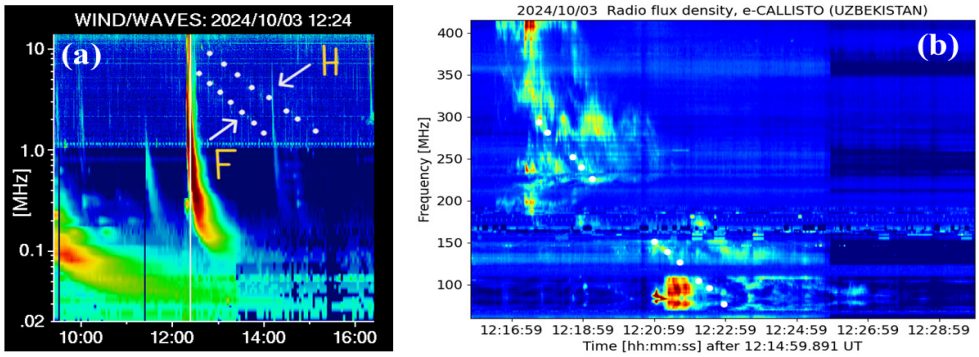


Figure 1 (a) IP type II burst with fundamental and harmonic emissions observed in the frequency range of 1–14 MHz by the Wind/WAVES instrument on 3 October 2024, with onset at ∼ 12:10 UT. (b) Dynamic spectrum of the type II burst recorded by e-CALLISTO (Uzbekistan) at ∼12:18 UT on October 3 2024.

frequencies below 1 MHz also included the low frequency group, which generated a burst that amplified to a distance of more than ∼45 $R_\odot$. They found that 37% and 12% of the low frequency group events produced shocks greater than 0.5 a.u in SC cycles 23 and 24, respectively. Joshi et al. (2024) observed that 45% of type II radio bursts in the SC 23, 24, and ascending phase of SC 25 correspond to frequencies of 13–14 MHz, and 12% are above 15 MHz.

In our study, with reference to the total of the 705 IP type II bursts, 30 (4.3%) were not associated with CMEs, while 675 (96%) were associated with CMEs. Out of 675 CMEs, 204 are attributed to Halo CMEs. Out of all of the IP type II bursts, two are double type II bursts and are caused by CME–CME interactions. The total number of IP type II bursts was caused by B-class (5), C-class (138), M-class (275), and X-class (124) solar flares. During the descending phase of SC 23, the influence of X and M class flares in generating type II bursts increased, while during the descending phase of SC 24, flares were relatively less dominant. The relationship between the CME and the shock wave is confirmed by the detection of an IP type II burst observed on October 3, 2024, by the WIND/WAVES (Fig. 1a). This radio burst was caused by X9.0 class soft X-ray solar flare observed by the X-ray sensor onboard Geostationary Operational Environmental Satellite (GOES) from the NOAA 13842 active region on the south-western solar disk at 12:15 UT and Uzbekistan CALLISTO instrument detected at 12:20 UT (Fig. 1b). The first height–time measurement of the CME was at $t_1 = 12 : 48$ UT when it is leading edge (LE) was located at $r_1 = 3.89\ R_\odot$ in the Large Angle and Spectrometric COronagraph (LASCO) field of view (FOV). It is an average speed and acceleration of the CME between first and last observed location (3.89 $R_\odot$ and 15.84 $R_\odot$) in the LASCO FOV was 821 km/s and –17.2 m/s^2.

Kumari et al. (2023) studied the relationship between metric type II bursts and SC and CME parameters. They found that only 4% and 3% of total CMEs were accompanied with type II bursts in SCs 23 and 24, respectively. As can be seen from Fig. 2, the correlation between IP type II bursts and sunspots during the ascending

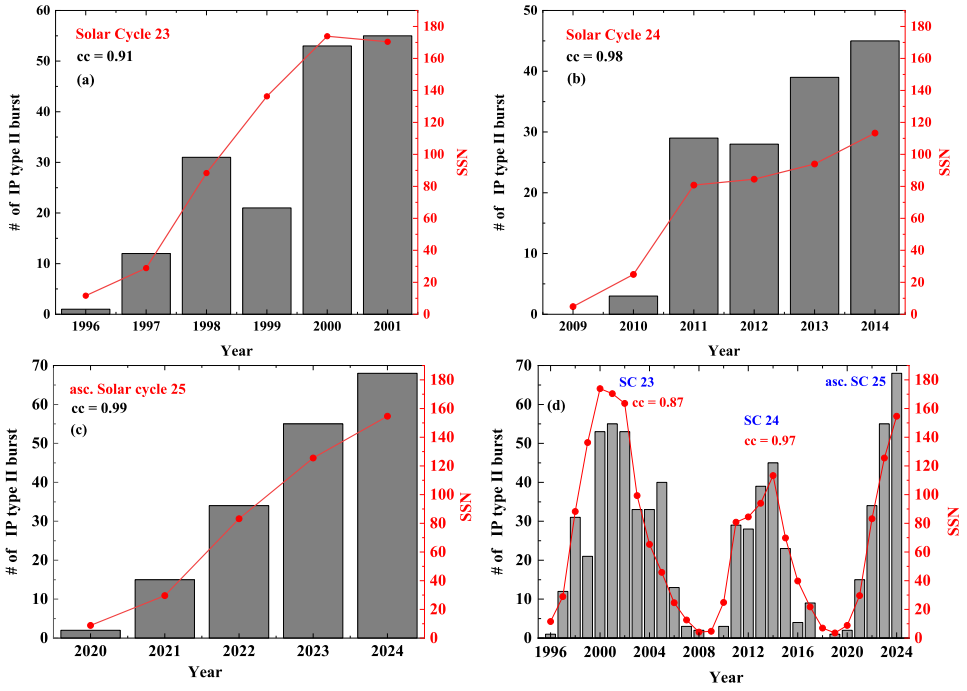


Figure 2 Four panels (a, b, c, d) show the occurrence rate of IP type II bursts (histograms) alongside SSN (red dotted line) during solar cycles 23, 24 and ascending phase of SC 25.

phase of SCs 23, 24 and 25 are presented and show a very strong correlation. Figure 2(a,b) shows a strong correlation (0.91, 0.98) between IP type II and SSN in SC 23 and 24, respectively. This is slightly lower than the correlation ($cc = 0.94$) reported in (Kumari et al. 2023). Interestingly, during the ascending phase of SC 25, the number of IP type II bursts accordingly increases with SSN ($cc = 0.99$, Fig. 2c). The relationship between the number of IP type II bursts and the SSN showed a higher correlation in cycle 24 than in cycle 23 (Fig. 2d). This correlation is almost similar to the relationship between type II bursts and SSN in Kumari et al. (2023).

Figure 3 presents the scatter plot showing the association of different flare classes (C, M, and X) that occur with IP type II radio bursts. Panels (a), (b) and (c) represent the dependence of the number of C, M and X class solar flares on the number of IP type II bursts, respectively. We can see that for the rising phase of SC 23, 24 and SC 25, IP type II bursts occurred with the most M-class solar flares (51%). These values were close to the values reported in (Patel et al. (2021), 45–55%) and (Joshi et al. (2024), 55%). We found that C and X class flares were associated with 25% and 23% of IP type II bursts, respectively.

The main reason for the strong association of IP type II bursts with M-class solar flares is that IP type II bursts are related to the plasma frequency, and they are observed as a frequency shift as the shock waves travel through the corona. M-class or X-class flares have enough energy to produce fast CMEs which are capable of driving shock waves. C-class flares are less likely to produce fast CMEs, therefore

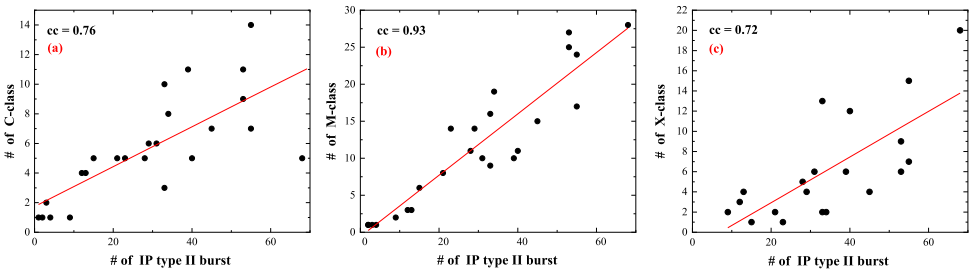


Figure 3 Scatter plot showing the number of flares by class dependence to IP type II burst number. Panels (a), (b) and (c) represent the dependence of the number of C, M and X class solar flares on the number of IP type II bursts, respectively.

stronger flares (M- and X-class) are even more likely to be associated with IP type II bursts. But M-class flares occur more frequently then X-class flares, therefore IP type II bursts are strongly correlated with M class bursts. Bhat et al. (2016) also studied the correlation of Halo CMEs with solar flare classes in with and without DH type II bursts from 1996 to 2008. M-class solar flares showed a correlation of 29% in the with DH type II bursts and 16% in without of DH type II bursts.

The role of flare geometry and CME direction is critical in determining the shock's propagation path, its interaction with the ambient medium, and thus the burst's detectability and spectral properties. CMEs that originate near the Sun's disk center (called "disk CME" within 45 degrees) travel approximately along the Sun–Earth line, making frontside halo CMEs highly likely to impact Earth. In contrast, frontside limb CMEs, originating from longitudes between 45 and 90 degrees, travel at an angle to the Sun–Earth line, resulting in only a partial impact on Earth's magnetosphere (Gopalswamy et al. 2007).

4 Conclusion

In this study, we conducted a detailed examination of IP type II radio bursts occurring during solar cycles SC 23, 24 and the ascending phase of SC 25, covering a total of 705 IP type II bursts from January 1996 to September 2024. The number of IP type II bursts is consistent with the periodic behavior of the solar cycle, but there are differences in the duration of the events (Fig. 2). This is important for understanding solar activity and its implications for the corona and heliosphere.

We found that 275 (50%) of IP type II bursts were associated with M-class solar flares, 138 (25%) with C-class solar flares, and 124 (23%) with X-class solar flares. We examined the correlation of IP type II burst numbers with SSN during the ascending phase of all three SCs, and the ascending phase of SC 25 currently shows the strong correlation ($cc = 0.99$). In the correlation between IP type II bursts and flare class, we found that M-class solar flares showed a higher correlation. This suggests that M-class solar flares are the main cause of IP type II bursts.

Acknowledgements

We gratefully acknowledge the WIND/WAVES type II burst catalog. The LASCO CME catalog is generated and maintained at the CDAW Data Center by NASA and The Catholic University of America in cooperation with the Naval Research Laboratory.

References

Bhatt, B., Prasad, L., et al. 2016. Astrophys. Space. Sci., Vol. 361, Issue 8, 8 pp.
Gopalswamy, N., Makela, P., et al 2015, URSI AT-RASC, 1–1 pp.
Joshi, B., Patel, B., et al. 2024, IAU Symp. Number 388.
Kumari, A., Morosan, D. E., et al. 2023, A&A, Vol. 675, 11 pp.
Patel, B., Joshi, B., et al. 2021, Sol. Phys., Vol. 296, Issue 9, 142 pp.
Pick, M. & Vilmer, N. 2008, Astron. Astrophys. Rev., Vol. 16, 1–153 pp.
Webb, D. F. & Howard, T. A. 2012, Liv. Rev. Sol. Phys., Vol. 9, Issue 1, 83 pp.
Gopalswamy, N., Yashiro, S., & Akiyama, S. 2007, J. Geophys. Res. Vol. 112, A06 112 pp.